

## Simulation and Verification of Cu@Ag Core-shell Sintered Paste for Power Semiconductor Die-attach Applications

Wang, Xinyue ; Zeng, Zejun ; Zhang, Jing ; Zhang, Guoqi; Liu, Pan

**DOI**

[10.1109/ECTC51906.2022.00086](https://doi.org/10.1109/ECTC51906.2022.00086)

**Publication date**

2022

**Document Version**

Final published version

**Published in**

Proceedings of the 2022 IEEE 72nd Electronic Components and Technology Conference (ECTC)

**Citation (APA)**

Wang, X., Zeng, Z., Zhang, J., Zhang, G., & Liu, P. (2022). Simulation and Verification of Cu@Ag Core-shell Sintered Paste for Power Semiconductor Die-attach Applications. In L. O'Conner (Ed.), *Proceedings of the 2022 IEEE 72nd Electronic Components and Technology Conference (ECTC)* (pp. 507-512). Article 9816740 (Proceedings - Electronic Components and Technology Conference; Vol. 2022-May). IEEE. <https://doi.org/10.1109/ECTC51906.2022.00086>

**Important note**

To cite this publication, please use the final published version (if applicable). Please check the document version above.

**Copyright**

Other than for strictly personal use, it is not permitted to download, forward or distribute the text or part of it, without the consent of the author(s) and/or copyright holder(s), unless the work is under an open content license such as Creative Commons.

**Takedown policy**

Please contact us and provide details if you believe this document breaches copyrights. We will remove access to the work immediately and investigate your claim.

***Green Open Access added to TU Delft Institutional Repository***

***'You share, we take care!' - Taverne project***

**<https://www.openaccess.nl/en/you-share-we-take-care>**

Otherwise as indicated in the copyright section: the publisher is the copyright holder of this work and the author uses the Dutch legislation to make this work public.

# Simulation and Verification of Cu@Ag Core-shell Sintered Paste for Power Semiconductor Die-attach Applications

Xinyue Wang  
Academy for Engineering and  
Technology  
Fudan University  
Shanghai, China  
(First Author)

Zejun Zeng  
Academy for Engineering and  
Technology  
Fudan University  
Shanghai, China

Jing Zhang  
Heraeus Materials Technology  
Shanghai Ltd.  
Shanghai, China

Guoqi Zhang  
Electronic Components,  
Technology, and Materials  
Delft University of Technology  
Delft, the Netherlands

Pan Liu  
Academy for Engineering and  
Technology; Fudan University  
Shanghai, China;  
Yiwu Research Institute of Fudan  
University; Research Institute of  
Fudan University in Ningbo  
panliu@fudan.edu.cn  
(Corresponding Author)

**Abstract**—With the increasing application of wide bandgap materials such as silicon carbide and gallium nitride in power devices, the working temperature of power devices has been pushed further. Therefore, it brings higher requirements for packaging materials. Sintered silver is a widely accepted chip connection material. However, silver suffers from high prices and electromigration. Therefore, a novel sintered material based on silver-copper core-shell structured particles raises the attention of researchers to solve this deficiency. To accelerate the development of new materials and their related processes, a four-sphere model of the silver-coated copper structure is established in this paper. The mathematical relationship between the porosity and thermal conductivity of sintered body and the actual sintering process was preliminarily established through the calculation based on a series of FEM simulations. The model was further validated through experiments. The modeling method and conclusion are utilized for future process adjustment, which is of great significance to accelerate the development, application, and reliability of new packaging materials.

**Keywords**—die-attach material; power electronic packaging; simulation; Cu@Ag particles

## I. INTRODUCTION

With the development of wide bandgap semiconductor devices, relevant packaging materials have been developed for high temperature, high frequency, and high power applications[1], such as silver sintering materials. However, due to the high cost of sintered silver and the problem of electromigration, novel solutions have been emerging such as copper sintering[3], surface modified metal particles, etc. The development of surface modification techniques have been introduced, e.g., silver-coated copper (Cu@Ag core-

shell) particles[4], which have great potential to provide reliable die-attach for power semiconductors.

During the process of developing such novel materials, computational simulation methods are helpful to optimize and simplify the exploration of sintering paste composition and sintering process parameters. Most of the existing sintering simulation studies focused on molecular dynamics simulations, which presented the movement of thousands of atoms through a large number of calculations and simulated clusters of silver atoms with a diameter of typically 1-5 nanometers[7]. However, most materials in the actual sintering process are micro-nano particles (above 100nm). Therefore, it is difficult to carry out molecular dynamics simulation and get a conclusion combined with the actual results. To solve this problem, the Finite Element Method (FEM) was utilized to simulate the process of sintering. The results obtained confirmed the changes in heating rate, holding time, and other parameters in the actual process, which provided that the finite element simulation method had the potential of assisting the development and prediction of the sintering process[8, 9].

In this work, we proposed a four-sphere model for predicting sintered materials development, which was a macroscopic model established through Finite Element Method (FEM) simulation in COMSOL Multiphysics software. The mathematical relationship between the porosity and thermal conductivity of sintered body and the actual sintering process (temperature, pressure, and sintering time) was preliminarily established through the calculation. The model was further validated by comparing with the experimental data of sintering paste composed Cu@Ag core-shell particles combined with the pressure sintering process. Such analysis is to accelerate the development of new

sintered materials and to improve the reliability of power semiconductor applications.

## II. SIMULATION MODEL DESCRIPTION

The finite element method (FEM) was applied to calculate the relationship between the porosity and the electrical/thermal conductivity of the sintered particles. The temperature distribution and potential distribution were analyzed. During sintering, the Cu@Ag particles come into contact to form sintered necks and further densification. Due to the different sintering process conditions, the porosity of the sintered material after densification will also be different. The existence of pores will inevitably affect the thermal conductivity and electrical conductivity of the sintered material. To study the electrical and thermal conductivity of the Cu@Ag paste under different sintering processes, a four-sphere model was established in this work to simulate the different porosity levels after sintering. A heat source and an electric current are respectively applied across the sintered body to establish the temperature field distribution and potential distribution. Next, the electrical conductivity and thermal conductivity are calculated according to the field distribution. Finally, thermal and electrical conductivity changes with the porosity of the sintered Cu@Ag paste are further analyzed. The independent variable is the size of the contact between the particles, and the dependent variables are the changes in thermal conductivity and electrical conductivity.

For this purpose, COMSOL Multiphysics 5.6 software with the Heat Transfer in Solids Module and the AC/DC Module was applied. The geometrical design of the sintered system is shown in Fig. 1 and Table 1, while the material performance parameters of the model composition are shown in Table 2. A system consisting of four Cu@Ag particles with a diameter of 2  $\mu\text{m}$  was set up to simulate the actual sintered structure. The diameter of the set copper core is 1.5  $\mu\text{m}$ , and the thickness of the silver shell is set to 0.25  $\mu\text{m}$ . The mesh structure is illustrated in Fig. 2.

In this simulation work, to focus on the changes in electrical and thermal conductivity due to the degree of particle contact, the plastic deformation caused by particle

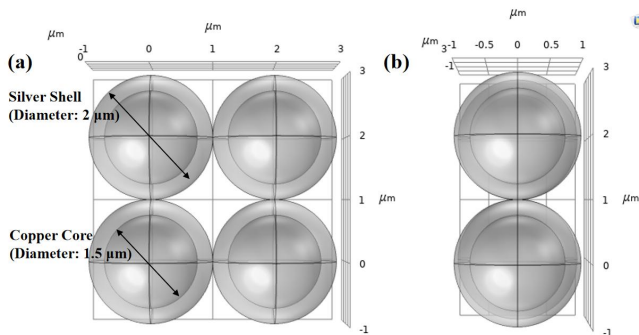


Figure 1. Schematic of the geometrical model: (a) main, (b) side view

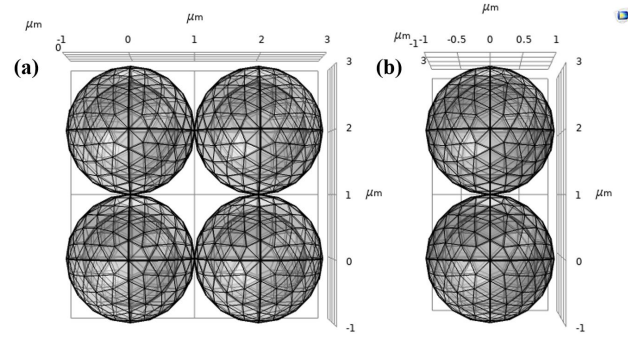


Figure 2. (a) main, (b) side view of the mesh structure of the model

TABLE I. GEOMETRY DESIGN PARAMETERS

Parameter	Material	Diameter ( $\mu\text{m}$ )
Core	Copper	1.5
Shell	Silver	2

TABLE II. MATERIAL PROPERTIES

Material properties	Material	
	Silver	Copper
Density ( $\text{kg.m}^{-3}$ )	10.53	8.96
Thermal conductivity ( $\text{W.m}^{-1}\text{.K}^{-1}$ )	426	400
Constant pressure heat capacity ( $\text{J.kg}^{-1}\text{.K}^{-1}$ )	234	386
Electrical conductivity ( $\text{S.m}^{-1}$ )	$6.3 \times 10^7$	$5.9 \times 10^7$

extrusion and material migration around the sintered neck were ignored. Simplified assumptions were made to focus on the changes in porosity. Meanwhile, the formulas for calculating the porosity from the model were also evaluated.

The variation of porosity was simulated by adjusting the contact length of the sintered neck between the individual particles. The particle radius is  $R$ , the sintering neck width between two particles is  $2x$ , and the distance from the particle sphere center to the sintering contact surface is  $d$ , as shown in Fig. 3. Therefore, its geometric relationship can be shown as equation (1).

$$d^2 = R^2 - x^2 \quad (1)$$

Then, the porosity( $P$ ) can be derived as follows:

$$1 - P = \frac{4V_{\text{Sphere}} - 24V_{\text{Spherical cap}}}{V_{\text{Cubic}}} \quad (2)$$

$$= \frac{4 \times \frac{4}{3} \pi R^3 - 24 \times \pi \left( \frac{2}{3} R + \frac{1}{3} d \right) (R - d)^2}{4d \times 4d \times 2d}$$

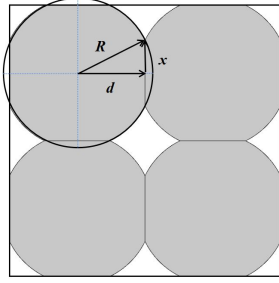


Figure 3. Orthographic view of the model after sintering

Bring Equation (1) into the above equation to calculate the relationship between porosity ( $P$ ) and neck diameter ratio ( $x/R$ ):

$$1 - P = \frac{3\pi}{4 \left[ 1 - \left( \frac{x}{R} \right)^2 \right]} - \frac{\pi}{3 \left[ 1 - \left( \frac{x}{R} \right)^2 \right]^{\frac{3}{2}}} - \frac{\pi}{4} \quad (3)$$

$$P = 1 - \frac{3\pi}{4 \left[ 1 - \left( \frac{x}{R} \right)^2 \right]} + \frac{\pi}{3 \left[ 1 - \left( \frac{x}{R} \right)^2 \right]^{\frac{3}{2}}} + \frac{\pi}{4} \quad (4)$$

Finally, the relationship between  $P$  and  $x/R$  is shown in Equation (4), which will be employed in the analysis of thermal and electrical conductivity variety in the following Section III. Through Equation (4), it is clear that as the  $x/R$  value increases, the porosity gradually decreases.

### III. SIMULATION RESULTS

#### A. Thermal conductivity

Thermal conductivity ( $\kappa$ , W/m.k) is a description of the ability of an object to conduct heat and is critical to packaging materials, especially die-attach materials. Its derived formula comes from Fourier's law, which is defined as the heat transferred by unit temperature gradient through unit heat conduction surface in unit time, as shown in Equation (5).

$$Q = \frac{\kappa A \Delta T}{L} \quad (5)$$

Where  $Q$  is heated,  $A$  is the contact area,  $L$  is heat transfer distance, and  $\Delta T$  is the temperature difference.

In this work, we set the top face of the model as the hot end (heat source,  $q=5 \times 10^9$  W/m<sup>2</sup>), and the bottom face as the cold end (fixed at 273.15 K). First, the temperature gradient is calculated through Heat Transfer in the Solids Module of the COMSOL. Next, Equation (5) is combined

with the existing model to deduce the expression of thermal conductivity:

$$\kappa = \frac{QL}{A\Delta T} \approx \frac{(q \times 2\pi r^2)Ad}{(2d \times 4d)\Delta T} \approx \frac{q\pi r^2}{d\Delta T} \quad (6)$$

Then, the calculated temperature difference was brought to Equation (6) to calculate the thermal conductivity under the current porosity. Finally, the size of the contact between particles ( $x/R$ ) was changed to obtain the temperature distribution and the equivalent thermal conductivity of the sintered body under different porosity. The results are established in Fig. 4 and Fig. 5. Since the copper core contact is not considered, we calculated the value of  $x/R$  in the interval of 0 to 0.65.

As shown in Fig. 4, the thermal conductivity ( $\kappa$ ) of the model has a good linear relationship with  $x/R$ . With the increase of the  $x/R$  value, the porosity gradually decreases and the thermal conductivity increases gradually. When  $x/R$

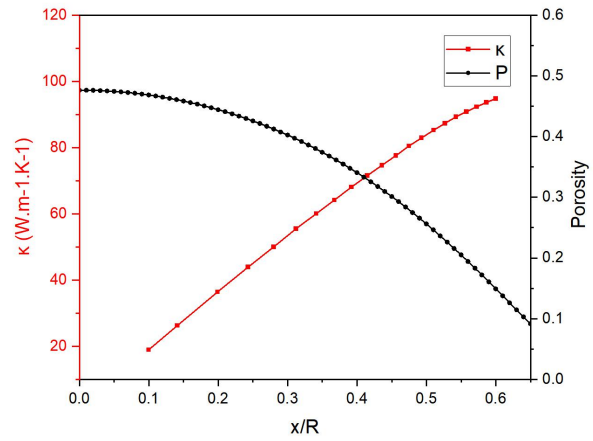


Figure 4. Simulation results of thermal conductivity with different porosity

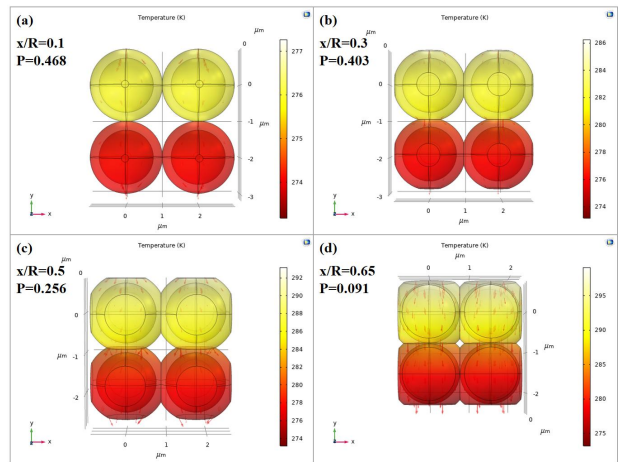


Figure 5. Temperature distribution of sintered body with different porosity

reaches 0.65, the copper core is close to contact, and the simulated thermal conductivity is approximately 94.8 W/m.k, which is about a quarter of the thermal conductivity of bulk copper. Combined with the temperature distribution results of different porosity, as shown in Fig. 5, as the particles approach, the pores of the four-sphere system gradually shrink and are similar to the bulk. The overall temperature distribution is also more uniform, in line with the calculated trend of increasing thermal conductivity.

### B. Electrical conductivity

Similar to the thermal conductivity, electrical conductivity ( $\sigma$ ) is a parameter used to describe the ease of charge flow in a substance and is another important performance indicator of die-attach materials. According to the definition, the calculation formula of conductivity can be obtained as Equation (7):

$$\sigma = \frac{J}{E} \quad (7)$$

Where  $J$  is the current density and  $E$  is the electric field strength.

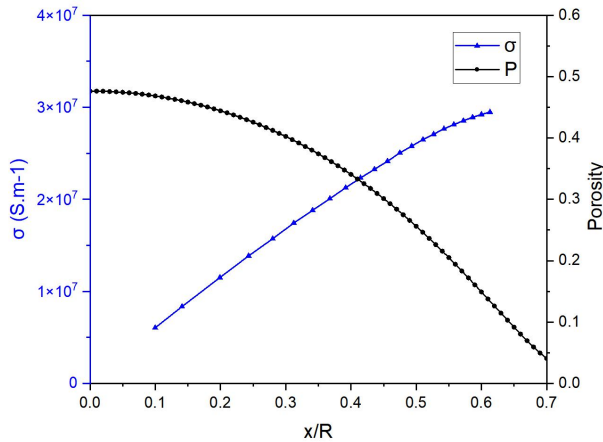


Figure 6. Simulation results of electrical conductivity with different porosity

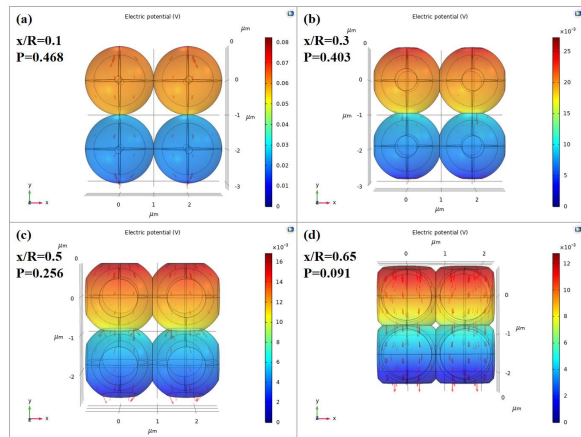


Figure 7. Potential distribution of sintered body with different porosity

In this simulation, we set the current injected at the top face to be 1 A, and the bottom face to be grounded in the AC/DC Module of the COMSOL software. Therefore, the distribution of the system potential can be obtained through calculation. Next, combined with Equation (7), the formula for calculating conductivity can be derived, as Equation (8):

$$\sigma = \frac{J}{E} = \frac{LI}{A\Delta U} \approx \frac{4d \times I}{(2d \times 4d)\Delta U} \approx \frac{I}{2d\Delta U} \quad (8)$$

Where  $\Delta U$  is the potential difference, and the value can be obtained by the probe. Then, the size of the contact between particles ( $x/R$ ) was changed to obtain the potential distribution and the equivalent electrical conductivity of the sintered body under different porosity. The results are shown in Fig. 6 and Fig. 7.

As the porosity decreases, the electrical conductivity gradually increases, as shown in Fig. 6. However, as the value of  $x/R$  increases, the increase in conductivity gradually becomes slower. When  $x/R$  is close to 0.65, the conductivity reaches  $2.98 \times 10^7$  s/m, which is half that of pure copper bulk. The potential distribution diagrams under different porosity are shown in Fig. 7. With the shrinking of the pores, the uniformity of the potential distribution is significantly improved, which is consistent with the conclusion in Fig. 6.

### IV. VALIDATION

To validate the model for sintered Cu@Ag particles, a sinter paste consisting of Cu@Ag particles and solvent was prepared. Commercialized Cu@Ag particles with an average diameter of 1~3  $\mu\text{m}$  were chosen, the scanning electron microscope (SEM) photo is shown in Fig. 8. In addition, the alcohol-based solvent was prepared, making up 15% of the total weight of the paste, and the configuration process is shown in Fig. 9(b). The agate mortar combined with a centrifuge was applied to the mixing of particles and the solvent.

After preparing the sintering paste, to test the porosity and corresponding thermal and electrical conductivity of the sintered layers produced under different processes, flakes sintered under different pressures were prepared. As shown in Fig. 9(c), after stencil printing on ceramic substrates,

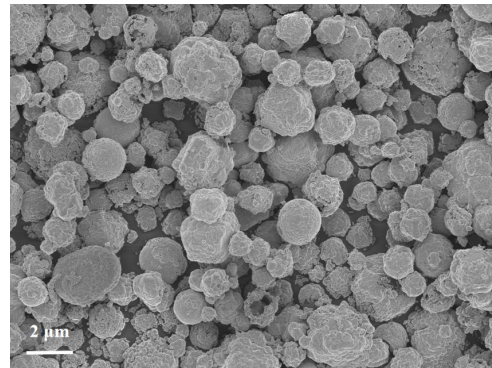


Figure 8. SEM photo of Cu@Ag particles

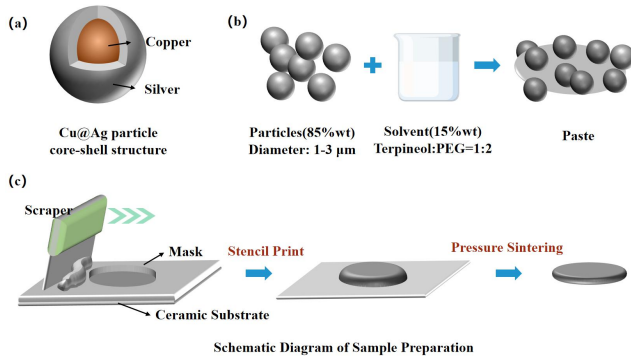


Figure 9. Schematic diagram of (a) core-shell structure, (b) paste preparation, (c) sample preparation

samples were sintered in the nitrogen atmosphere under the pressure of 5 MPa, 10 MPa, and 15 MPa, respectively, at 250°C for 600 s, using Boschman Sinterstar Innovate-F-XL. Then, flake samples were fabricated with approximately 12.7 mm in diameter and 0.5~1.5 mm in thickness. Subsequently, a laser thermal conductivity testing instrument (LFA 467) was applied to analyze thermal conductivity under (25±5)°C, (30~70)%RH. The laser voltage was selected as 250.0 V with a pulse width of 0.30 ms. And a four-probe tester (RTS-8) was utilized to analyze electrical conductivity under (25±5)°C, 65%RH. SEM combined with ImageJ software was applied to obtain the porosity of the sintered flakes. The test results are shown in Fig. 10 and Table 3.

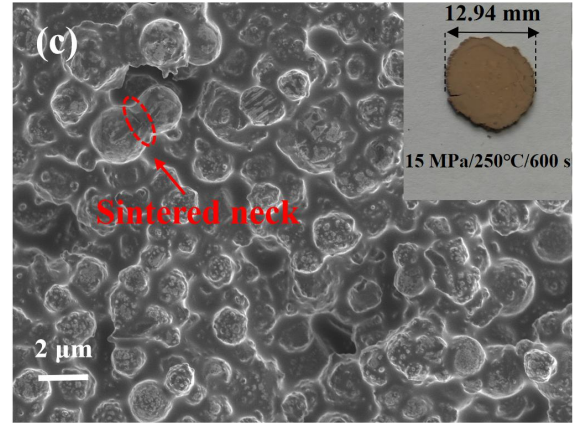
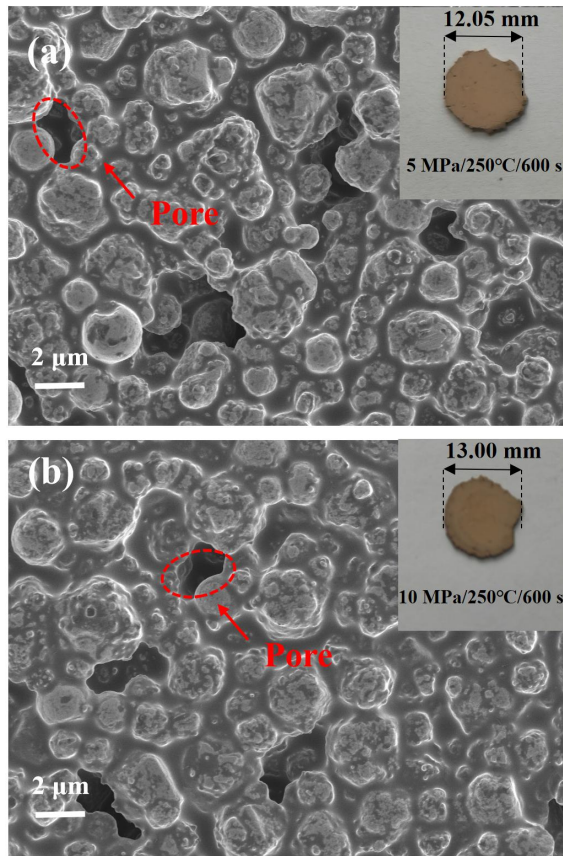


Figure 10. SEM photos of the flake samples (a) 5 MPa, (b) 10 MPa, (c) 15 MPa

TABLE III. ACTUAL MEASURED MATERIAL PROPERTIES

Average Properties	Samples		
	5 MPa	10 MPa	15 MPa
Porosity	0.412	0.292	0.067
Density (kg.m <sup>-3</sup> )	5.35	5.57	5.66
Thermal conductivity (W.m <sup>-1</sup> .K <sup>-1</sup> )	47.27	61.66	94.18
Simulated Thermal conductivity (W.m <sup>-1</sup> .K <sup>-1</sup> )	50.01	77.58	--
Electrical conductivity (S.m <sup>-1</sup> )	0.84×10 <sup>7</sup>	1.12×10 <sup>7</sup>	1.40×10 <sup>7</sup>
Simulated Electrical conductivity (S.m <sup>-1</sup> )	1.57×10 <sup>7</sup>	2.41×10 <sup>7</sup>	--

It is worth mentioning that the porosity of the plane will be different from the porosity of the three-dimensional. Therefore, after obtaining the porosity from the SEM photos, we obtained the stereo porosity through the mathematical calculation, which were used for the comparison in Table 3.

Compared with the simulation results, the thermal conductivity and electrical conductivity in the actual test are higher. Though maintaining the same trends of changing with porosity, tested electrical conductivity values are deviated more from simulated results due to the porosity influence. Combined with the model simplification assumptions and the analysis of Fig. 10, the main reasons are as follows: (1) With the reduction of porosity, in addition to the sintered connection formed by the silver shell layer, the contact of copper cores was also found at 15 MPa. (2) During the sintering process, the silver in the sintered neck will migrate to the outside, but the transport of this part of the material is not considered in the model. (3) The contact layer between the copper core and the silver shell and the contact between the particles will change the phase and lattice of the materials, thus reducing the thermal and electrical conductivity of the system.

According to the actual test results, the simulation model still needs to be further improved, such as the thin-layer

design of the inter-particle contact interface and the copper-silver interface. The parameter adjustment of the thin layer material refers to the material properties of the corresponding alloy. Based on such a calibration model, the material transport around the sintered neck and the contact of the copper core can be further evaluated to reduce the deviation. Further work will be focused on lifetime prediction combining reliability tests and multi-physics simulations by utilizing this novel paste on Direct Bond Copper (DBC) substrate with SiC chips.

## V. CONCLUSIONS

In this work, a sintering simulation model based on Cu@Ag core-shell particles for power semiconductor die-attach applications was introduced. Through adjusting the contact scale between the four spheres, the temperature distribution and potential distribution of the system under different porosity are obtained. The variation trends of thermal conductivity and electrical conductivity of the four-sphere system under different porosity are analyzed. Flakes with different porosity were obtained via adjusting the sintering pressure and using the sintering paste prepared in the laboratory.

The model was further validated by comparing with the experimental data of sintering paste composed Cu@Ag core-shell particles combined with the pressure sintering process. The experimental results illustrated that with the increase of sintering pressure, the  $x/R$  value of the sintered neck between particles increases, the porosity gradually decreases, and the electrical and thermal conductivity increases. However, the values simulated by the model are all higher than actual values, especially for electrical conductivity, which is probably due to the neglected particle contacts and silver-copper contact layers. Meanwhile, the mass transport around the sintered neck and the copper core contact also need to be further considered to optimize the model.

The modeling method and conclusion can be utilized for the process adjustment in the subsequent sintering work, especially for novel materials such as Cu@Ag particles, which is of great significance to the actual production and product development to accelerate the development of new sintered materials and to improve the reliability of power semiconductor applications.

## ACKNOWLEDGMENT

In this work, the authors would like to thank the Key-Area Research and Development Program of Guangdong Province (2020B010170002), Shanghai SiC Power Devices Engineering & Technology Research Center (19DZ2253400), Yiwu Research Institute of Fudan University (20-1-03), and Research Institute of Fudan University in Ningbo for funding this research and providing simulation support and laboratory accesses. Many thanks to Heraeus Materials Technology Shanghai Ltd. for prototype validation and characterization, and Mr. Zhou Dong Yang, Mr. Hanyan Gao, graduate students from Fudan University for characterization support, respectively.

## REFERENCES

- [1] V. R. Manikam and K. Y. Cheong, "Die Attach Materials for High-Temperature Applications: A Review," *Ieee Transactions on Components Packaging And Manufacturing Technology*, vol. 1, no. 4, pp. 457-478, Apr 2011.
- [2] M. Maruyama, R. Matsubayashi, H. Iwakuro, S. Isoda, and T. Komatsu, "Silver nanosintering: a lead-free alternative to soldering," *Applied Physics A*, vol. 93, no. 2, pp. 467-470, 2008.
- [3] Z. Wu, C. Jian, W. Qian, and J. Wang, "Low temperature Cu-Cu bonding using copper nanoparticles fabricated by high pressure PVD," *AIP Advances*, vol. 7, no. 3, p. 035306, 2017.
- [4] K. Zhao, T. Zhang, Y. Liu, and F. Sun, "Preparation of nano Cu@Ag core-shell powder for electronic packaging," in *2017 18th International Conference on Electronic Packaging Technology (ICEPT)*, 2017.
- [5] Y. Yong et al., "Use of decomposable polymer-coated submicron Cu particles with effective additive for production of highly conductive Cu films at low sintering temperature," *Journal of Materials Chemistry C*, vol. 5, 2017.
- [6] Y. Zhang et al., "Low temperature sintering-bonding using mixed Cu+Ag nanoparticle paste for packaging application," 2012.
- [7] H. Wang, D. Yang, M. Cai, X. Wang, and Z. Liang, "Thermal Simulation Modeling of IGBT Module Using Silver Nanoparticle Sintering Material," 2018, pp. 904-907.
- [8] Tan, S. Zhang, X. Zhao, Z. Wu, Z. and Z. H., "System simulation of multi-physical field coupling in electric current-assisted sintering," *Powder Metallurgy Technology*, vol. 38, no. 6, pp. 414-422, 2020.
- [9] B. Zhang, Y. Carisey, A. Damian, R. H. Poelma, and H. Zeijl, "3D interconnect technology based on low temperature copper nanoparticle sintering," in *International Conference on Electronic Packaging Technology*, 2016.